Observations of Continental Shelf Waves off Oregon and Washington

WILLIAM W. HSIEH[1]

Department of Oceanography, University of British Columbia, Vancouver, B.C., Canada V6T 1W5

(Manuscript received 9 December 1981, in final form 12 April 1982)

ABSTRACT

The low-frequency current fluctuations on the Oregon shelf changed dramatically from winter to spring, 1975. A much faster offshore energy decay occurred simultaneously with a sharp decrease in the alongshore propagation speed. Cross-shelf analysis in a frequency band around 0.16 cpd showed the emergence of the third-mode shelf wave in spring from the predominantly first-mode motion in winter. At frequencies < 0.1 cpd, the current fluctuations propagated southward in winter, opposite to the direction of shelf waves.

On the Oregon and Washington shelves during summer (and early fall) 1972, the location of moorings on irregular topography rendered data interpretation difficult. Nevertheless, the general cross-shelf and alongshore properties of the current fluctuations were consistent with the first-mode shelf wave, in contrast to the situation during summer 1973 when the second mode was excited.

The excitation of relatively high modes and the generally sharp concentration of energy in one particular mode are surprising and difficult to explain with the present shelf-wave generation theories. Nonlinear resonance between wind and current is proposed as a possible explanation.

1. Introduction

In the previous paper [Hsieh (1982); henceforth referred to as H1], a cross-shelf fitting of the theoretical shelf-wave current ellipses to the observed current ellipses clearly showed the second mode to be excited on the Oregon shelf during the summer of 1973. However, the low-frequency current fluctuations off Oregon are known to change with time. Investigating seasonal differences in the low-frequency current fluctuations on the Oregon shelf, Huyer *et al.* (1978) found that the offshore length scale for the coastally confined current fluctuations was about twice as great in winter (early 1975) as it was in the following spring, and that the length scale during summer 1973 lay somewhere between these two extremes. Since the offshore energy decay rate for a shelf wave depends on the mode number, can the observed changes in the offshore length scale merely reflect the excitation of different shelf wave modes at different times?

The alongshore propagation speed of these current fluctuations was found by Kundu and Allen (1976) to vary drastically—from 500 km day^{-1} northward during summer 1972 to 120 km day^{-1} northward during summer 1973. As the alongshore phase speed of a shelf wave is modal dependent, is this observed change in speed also an indication of different modes being excited at different times? If one can obtain from the alongshore phase speed, an estimate as to which mode is being excited, and from the cross-shelf structure, a second estimate, will the two estimates agree? These interesting questions are investigated in this paper, using the shelf-wave detection techniques developed in H1.

Since the low-frequency current fluctuations on the Oregon shelf are generally quite coherent with the wind fluctuations, some researchers (e.g., Hickey, 1981a,b) believe that the current fluctuations are simply wind-forced waves rather than shelf waves. [In this paper, the term shelf wave is used for a wave that satisfies the shelf-wave dispersion relation, regardless of whether energy is being transferred to the wave by the wind. In contrast, a forced wave refers to a wave with the same angular frequency ω and wavenumber k as the wind disturbance above, as manifested in the theoretical study of Gill and Schumann (1974).] While some current signals (especially at very low frequencies) appeared not to be shelf waves, most signals, when their cross-shelf structures were scrutinized agreed well with shelf waves. The conclusion after analyzing several data sets collected at different seasons is that the change in character of the current fluctuations on the Oregon and Washington shelves can often be accounted for by the excitation of different shelf-wave modes at different times.

Fig. 1 shows data sets from the Oregon and Washington shelves. The winter and spring, 1975, Oregon shelf data (taken during the WISP experiment by the Oregon State University at Corvallis), are analyzed in Section 2, while the summer and early fall,

[1] Present affiliation: Department of Applied Mathematics and Theoretical Physics, University of Cambridge, Cambridge CB3 9EW, England.

0022-3670/82/080887-10$06.50

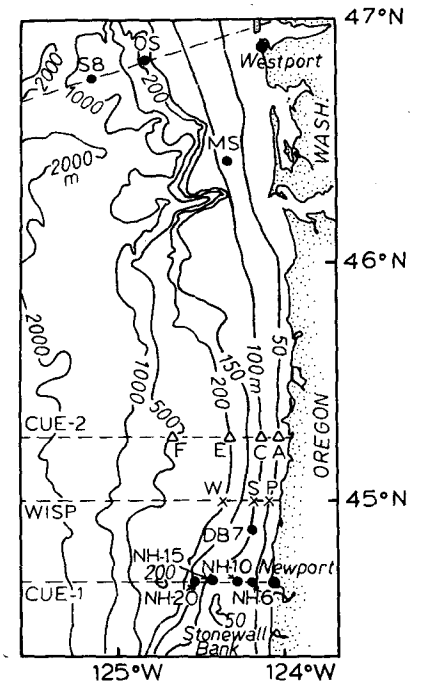

FIG. 1. Location of current meter moorings at various times on the Oregon and Washington shelves. The solid circles indicate the CUE-1 moorings off Oregon and the University of Washington moorings off Washington during summer and early fall, 1972. A, C, E and F label the CUE-2 moorings, Aster, Carnation, Edelweiss and Forsythia, during summer, 1973, while P, S and W stand for the WISP moorings Pikake, Sunflower and Wisteria, during winter and spring, 1975.

1972, data (collected on the Oregon shelf during the CUE-1 experiment by the Oregon State University, and on the Washington shelf by the University of Washington) are examined in Section 3. These data have been studied previously—the 1975 data by Huyer *et al.* (1978) and Hickey (1981a) and the 1972 data by Huyer *et al.* (1975), Kundu *et al.* (1975), Kundu and Allen (1976) and Hickey (1981b).

2. Winter and spring, 1975, Oregon shelf

The current-meter moorings Pikake, Sunflower and Wisteria (labelled P, S and W in Fig. 1) extended offshore in the WISP experiment. The data record for Pikake lasted from 28 January to 15 May 1975, while those for Sunflower and Wisteria, from 28 January to 26 April 1975. The onset of spring was determined in Huyer *et al.* (1978) to occur quite sharply at about 25 March. Data prior to, and data after this date, will be referred to as "winter" and "spring" data, respectively. The current records at 25 m are used here.

Fig. 2 shows the dispersion diagram consisting of the four lowest shelf-wave modes for the topography along the WISP array. Since there is no alongshore current meter array in WISP, we need to use the Newport adjusted sea level (inverse barometric effect and tides removed). Figs. 3a and 3b display the (inner) cross spectra between the current at Pikake and the Newport adjusted sea level during winter and spring, respectively.

The coherency at frequencies < 0.2 cpd (cycles per day) was higher in the winter than in the spring. Despite having similar record lengths and the same amount of band-averaging, the coherency spectrum in winter appeared more jagged than that in spring. Besides the high coherence at low frequency, peaks at around 0.33 and 0.5 cpd were also present. The 0.33 cpd signal seemed to strengthen in spring, while the 0.5 cpd signal weakened.

As in H1, if χ_- and χ_+ denote respectively the phase value for clockwise and anticlockwise motion at a certain frequency,

$$\delta_w = (\chi_- - \chi_+)/2 \qquad (1)$$

denotes the alongshore phase lag due to wave propagation, with δ_w positive when the second station leads the first (i.e., northward propagation). In winter, at very low frequencies ($\leq$0.1 cpd), $\chi_- < \chi_+$, implying a negative δ_w, and hence southward propagation at about 90 km day^{-1}. Above this very low frequency regime, the winter phase spectrum is quite linear with a small negative slope indicated by the dashed line. A linear relation between phase and frequency implies $k \propto \omega$, i.e., nondispersive propagation. A negative slope indicates northward propagation. From the slope, the phase speed c is estimated to be about 400 km day^{-1} northward, quite consistent with that of the first-mode shelf wave. (From Fig. 2, the nondispersive long-wave phase speeds for the first, second and third modes are determined to be 350, 120 and 55 km day^{-1}, respectively.)

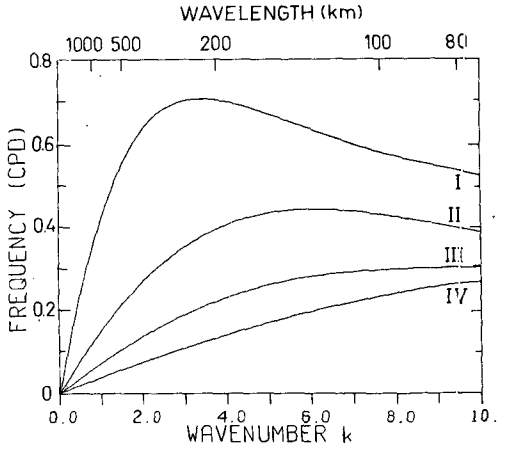

FIG. 2. Dispersion curves for the four lowest shelf-wave modes, integrated numerically along the topography of the WISP cross-shelf array (dashed line in Fig. 1). The wavenumber is nondimensionalized with respect to L^{-1}, where L = 120 km.

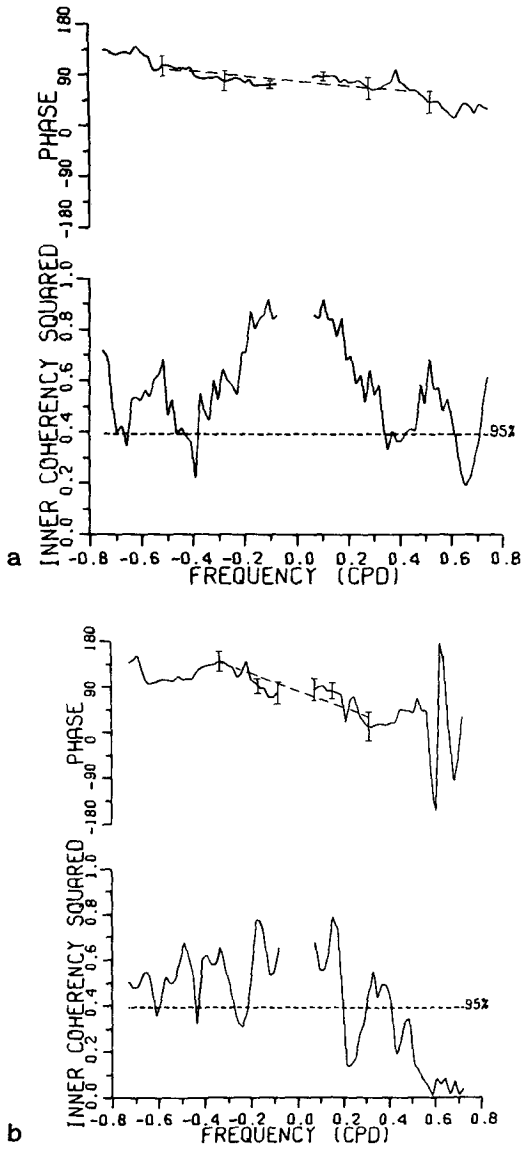

FIG. 3. Rotary (inner) cross spectra between the 25 m current at Pikake and the adjusted sea level at Newport during (a) winter and (b) spring, 1975. The negative and positive frequencies denote clockwise and anticlockwise motion respectively. The horizontal dashed lines in the coherency spectra indicate the 95% significance level. The 95% confidence limits for the phase spectrum (from Jenkins and Watts, 1968, Fig. 9.3) are shown for selected values.

In spring, the coherency at frequencies $\leqslant 0.1$ cpd dropped, and the resulting increase in the phase uncertainty made it impossible to determine whether there was still southward propagation at very low frequencies. However, for frequencies above this regime and below 0.3 cpd, the slope of the linear trend (Fig. 3b) becomes much steeper. As the slope is inversely proportional to the nondispersive phase speed, this indicates the northward propagation speed has dropped dramatically—from about 400 km day^{-1} in winter to about 90 km day^{-1} in spring—suggesting a possible change from a first-mode shelf wave to a higher mode one.

Let us examine the cross-shelf structure. Figs. 4a and 4b show the autospectra for the 25 m currents at the 100 m isobath station Sunflower (solid curves), and at the 200 m isobath station Wisteria (dashed curves) in winter and spring, respectively. One notices that at low frequencies, the offshore energy decay was much more rapid in spring than in winter. Also, at Wisteria, there appeared to be a general predominance of anticlockwise energy at all frequencies, especially in spring.

Table 1 displays the ratio of observed (anticlockwise, clockwise and total) energy at the 100 m isobath station to that at the 200 m isobath station, at low frequency (around 0.13 cpd). Since during summer 1973, the CUE-2 stations Carnation and Edelweiss were located at the 100 and 200 m isobaths close to the WISP stations, they are also included in the table. The theoretical values for modes 1, 2 and 3 (see Fig. 4b of H1) are listed for comparison. (The 25 m currents were used at Sunflower and Wisteria, 40 m at Carnation, and 80 m at Edelweiss.)

The table shows that (i) the offshore energy decay rates for the summer of 1973 were in excellent agreement with those of the second mode, (ii) the decay rates for winter 1975 were much slower than those

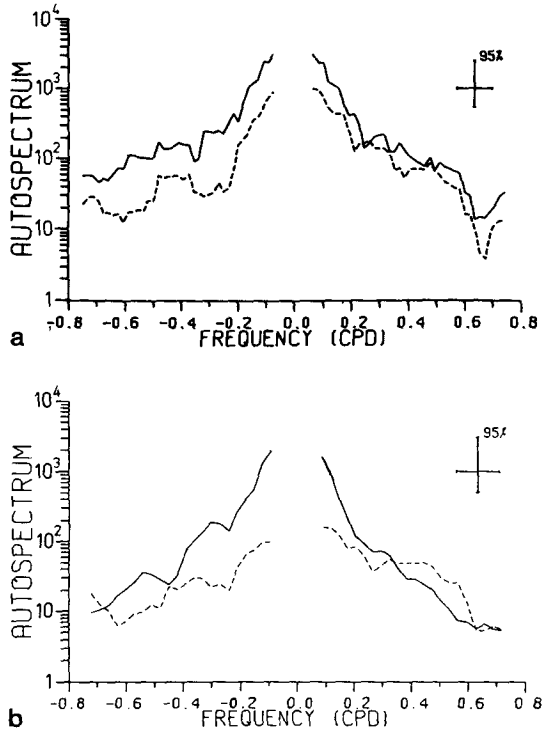

FIG. 4. Rotary autospectra between the 25 m currents at the 100 m isobath station Sunflower (solid curves), and the 200 m isobath station Wisteria (dashed curves), during (a) winter and (b) spring, 1975. The 95% confidence interval and bandwidth are as indicated.

TABLE 1. Ratio of energy between the 100 m isobath station and the 200 m isobath station at low frequency (~0.13 cpd). The theoretical values for modes, 1, 2 and 3 are listed for comparison. Mode 3 has nodes near the 200 m isobath (see Fig. 4b of H1); hence its ratios cannot be determined precisely.

Energy	Summer 1973	Winter 1975	Spring 1975	Mode 1	Mode 2	Mode 3
Anticlockwise	10.0	2.4	5.2	1.6	8.0	>5
Clockwise	5.2	3.3	12.0	1.5	4.7	>10
Total	6.7	2.8	7.7	1.5	5.7	>7

of the other two seasons and the two higher modes, and (iii) the rapid decay ratios for spring 1975 were consistent with those of the third mode.

Table 2 displays the ratio of clockwise energy to anticlockwise energy observed at various stations at low frequency, and the theoretical values for modes 1, 2 and 3. This table generally confirms the conclusions reached in Table 1. Furthermore, the observed predominance of anticlockwise energy at Wisteria during spring 1975 turned out to agree with the third mode which has considerably more anticlockwise energy at the 200 m isobath.

We next performed cross-shelf fitting of the theoretical shelf-wave current ellipses to the observed current ellipses, as in H1. Separate fits to winter and spring data were made at frequencies of 0.16, 0.33, 0.50 and 0.57 cpd. The observed current parameters were band-averaged with 14 degrees of freedom. [Kundu and Allen (1976) demonstrated that the current fluctuations aligned themselves along topographic contours. The contour at Wisteria was shifted by about 20° with respect to those at Sunflower and Pikake. This topographic phase shift was taken into account in the fitting.] Columns 2 and 3 of Table 3 list the properties of the shelf waves used in the fitting [the mode number and the wavelength λ (km)]. The deviation D is the residual of the fit divided by the total observed energy. If small, it indicates a good fit. When more than one shelf wave is fitted, the relative energy contribution of each wave is given in the column labelled $E_m/\Sigma E_m$.

During winter, a good fit (i.e., small deviation) occurred only in the frequency band centered around 0.16 cpd, where energy was present in the first and third modes, with the first mode dominating. But in spring, the dominance of the first mode yielded to the third mode. The relative energy contribution of the third mode to that of the first was 0.46:0.35. (This ratio is an average over the entire line of cross-shelf moorings, whereas in reality, the energy of the third mode is concentrated much closer to the shore. Therefore, near the coast, the third mode actually dominated over the first by a much larger ratio, but far enough offshore, the first mode would still contribute more energy than the third.) In the higher frequency bands around 0.33, 0.50 and 0.57 cpd, there was a general improvement in the fits, with the corresponding deviation values dropping from 0.71, 0.78 and 0.38 in winter, to 0.11, 0.24 and 0.34, respectively, in spring. Huyer *et al.* (1978) noted that although the alongshore current fluctuations were quasi-barotropic, the amplitude decreased with depth in winter, but remained quite uniform in summer. Hence the improvement in the fit (with a barotropic theory) during spring may have resulted from the decrease in the baroclinic fluctuations, which were large in winter.

The change in the current fluctuations (excluding the very low frequencies) from winter to spring, 1975, can be summarized as follows: In winter, even though the alongshore phase lag (Fig. 3a) indicated a generally nondispersive propagation at a phase speed comparable to that of the first mode, the cross-shelf current structures agreed well with the first mode only within a frequency band centered around 0.16 cpd. In spring, in the 0.16 cpd band, the third mode became dominant. This is supported by several pieces of evidence: 1) the slowing down of the alongshore propagation speed (Fig. 3b) at frequencies $\lesssim$ 0.3 cpd (note from Fig. 2 that the third mode cannot be excited above 0.3 cpd), 2) the rapid offshore decay in energy (Table 1), 3) the appropriate ratio of clock-

TABLE 2. Ratio of clockwise energy to anticlockwise energy observed at various isobaths at low frequency (~0.13 cpd). The theoretical values for modes 1, 2 and 3 are also listed for comparison. (Only during the summer of 1973 was there a mooring at the 500 m isobath. The 40 m current at Forsythia was used.)

Isobath (m)	Summer 1973	Winter 1975	Spring 1975	Mode 1	Mode 2	Mode 3
100	1.3	1.1	1.4	1.1	1.2	1.7
200	2.4	0.80	0.63	1.2	2.1	<1
500	0.72	—	—	1.4	0.5	2.9

TABLE 3. Cross-shelf modal fitting on the Oregon shelf at selected frequencies during winter and spring, 1975. The deviation D is a measure of the goodness-of-fit (small D implying good fit). The column $E_m/\sum E_m$ gives the relative energy contribution of the particular shelf wave in the fit.

Frequency (cpd)	Mode	λ (km)	Winter $E_m/\sum E_m$	Winter D	Spring $E_m/\sum E_m$	Spring D
0.16	1	2300	0.84	0.05	0.35	0.16
	2	700	0.01		0.19	
	3	310	0.15		0.46	
0.33	1	1000	0.81	0.71	0.83	0.11
	2	280	0.19		0.16	
0.50	1	580	—	0.78	—	0.24
0.57	1	470	0.73	0.38	0.78	0.34
	1	95	0.27		0.22	

wise to anticlockwise energy (Table 2), and 4) the result from cross-shelf modal fitting (Table 3). At frequencies > 0.3 cpd, the observed current fluctuations in spring improved their agreement with the first mode, probably as a result of the drop in the baroclinic current fluctuations.

The very low frequency (≤0.1 cpd) fluctuations propagated southward in winter, opposite to the direction of propagation observed at higher frequencies, and opposite to the direction of free shelf waves. This situation has been encountered previously on the Oregon shelf by Mooers and Smith (1968). Analizing data from the summer of 1933, they found a 0.1 cpd wave moving southward with the atmospheric pressure system, while a 0.35 cpd wave propagated northward as a free shelf wave. There are insufficient wind data in this study to determine whether the wind system was moving southward.

3. Oregon and Washington shelves, summer and early autumn, 1972

During the CUE-1 experiment, current meters were moored on the Oregon shelf (Fig. 1) from about 6 July to 30 August. The 60 m current meter at NH10 lasted until 18 September. The mooring NH6 was not deployed until early August and lasted well into autumn. On the Washington shelf, the current meter moorings MS, OS and S8 were deployed from 18 July to 24 September.

Kundu and Allen (1976, Fig. 8) noted a striking difference between the current fluctuations observed at 66 m depth at MS (or UWIN, in the notation of Kundu and Allen), and the fluctuations at 60 m at NH10. They found that for frequencies above 0.4 cpd, MS had much less energy than NH10. To investigate this phenomenon further, the two current records were decomposed into rotary components. Their autospectra are shown in Fig. 5, where we find that the shortage of higher frequency energy at MS

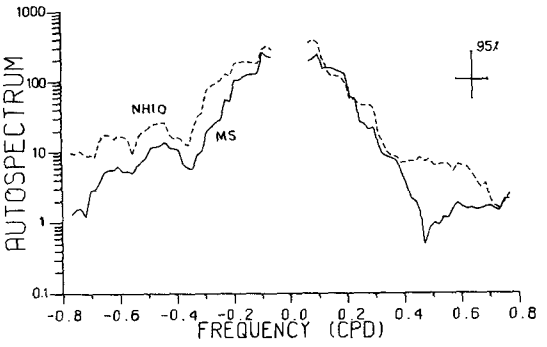

FIG. 5. Autospectra of the currents at MS (66 m) (solid line) and NH10 (60 m) (dashed line). Note the severe shortage of energy for anticlockwise motion at MS at frequencies between 0.4 and 0.6 cpd.

was really caused by a shortage of anticlockwise energy.

Fig. 6 (displaying the autospectra of the 60 m currents at MS, OS and S8) shows that on the Washington shelf, energy generally decreased offshore, but from 0.4 to 0.6 cpd, the anticlockwise energy at MS was less than those at OS and S8, stations much further offshore. This seems to imply that MS has been moored close to a node of the anticlockwise current fluctuations in the higher frequency regime of 0.4–0.6 cpd.

MS was moored 22 km from the shore. At frequencies > 0.4 cpd, only the first mode can be excited (Fig. 2). Fig. 4b of H1 illustrates that at 0.63 cpd, the node of the anticlockwise component occurred at around 60 km offshore for the first-mode long wave, but at around 20 km offshore for the first-mode short wave. Thus, the lack of anticlockwise energy in the higher frequency regime at MS is not incompatible with the presence of the first-mode short shelf wave. Short shelf waves, with group velocities opposite to their phase velocities, can be generated from long shelf waves either by scattering from irregular topography or by nonlinear resonant interactions.

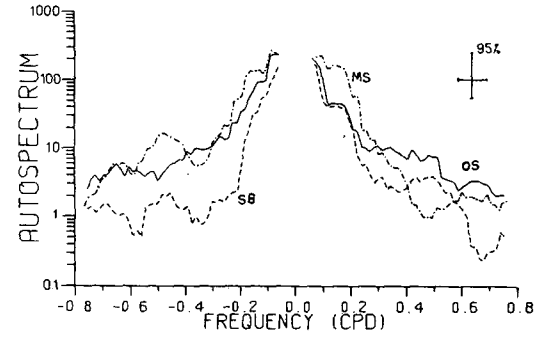

FIG. 6. Autospectra of the 60 m currents at MS, OS and S8, on the Washington shelf. (The curve for MS is not completely identical to that in Fig. 5 due to very slight differences in the starting time and in the length of the record used.)

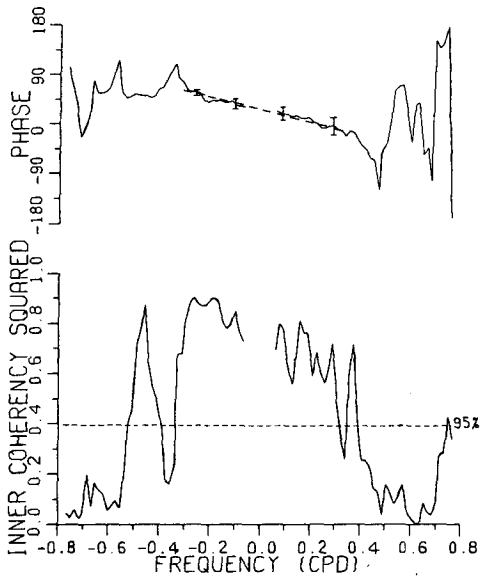

FIG. 7. Cross spectrum between the 60 m currents at MS and NH10.

The nonlinear interaction theory of Hsieh and Mysak (1980) does predict the presence of short shelf waves in a higher frequency regime. However, the irregular topography near MS, especially the canyon, may cause much wave-scattering.

Fig. 6 also shows that at low frequencies the offshore energy decay was quite slow in 1972, resembling Fig. 4a instead of Fig. 4b. The cross-spectrum between the 60 m currents at MS and NH10 is shown in Fig. 7. The phase spectrum shows a linear trend at low frequencies, indicating a northward nondispersive propagation speed of $\sim$600 km day^{-1}. Hickey (1981b) pointed out that this propagation speed was considerably higher than the 350–400 km day^{-1} nondispersive phase speed of the first-mode shelf wave, and interpreted the current fluctuations as forced waves.

We note from Fig. 1 that the topography is very complicated near MS and NH10. Wang (1980) showed that near topographic irregularities, the phase of a propagating shelf wave can be severely distorted. Since the phase speed was estimated using the phase lag between the two stations, distortion of phase at the stations could lead to an erroneous estimate of the phase speed. The lagged correlation study of Kundu and Allen (1976) showed a propagation speed of 500 km day^{-1} between MS and NH10, but for the stations located (in a region of more regular topography) between these two stations, the propagation speeds were considerably less, as shown in Fig. 10a of Kunda and Allen. Hence, it is possible that the apparently high phase speed between MS and NH10 was caused by topographic phase distortion at the two stations.

The mooring NH6 was installed on the Oregon shelf somewhat later than the other CUE-1 moorings, and remained in operation during the autumn. The cross-shelf spectrum between the 60 m current at MS and the 40 m current at NH6 (Fig. 8) reveals a phase spectrum that resembled those in Fig. 3. At low frequencies, there is a linear trend indicating northward propagation. But at very low frequencies, the phase values show $\chi_- < \chi_+$, and by Eq. (1), the propagation was southward. The records for MS and NH6 were then divided into two equal halves, and their cross spectra computed separately (not shown). The first half (mainly in August) showed no evidence of southward propagation, but the second half (mainly in September) displayed southward propagation at very low frequencies. Hence, it appeared that at very low frequencies, a southward propagation occurred in early fall, 1972, similar to the winter situation in 1975.

Table 4 shows the cross-shelf modal fitting on the Washington shelf during August–September 1972, while Table 5 shows the fitting on the Oregon shelf during July–August 1972. The 60 m currents at MS, OS and S8 were used for the fitting on the Washington shelf, while the 60 m current at NH10, and the 40 m currents at NH15 and NH20 were used for Oregon. The cross-shelf depth profiles used for computing the theoretical current ellipses were taken along the dashed line joining OS and S8 in Fig. 1, and along the dashed line labelled CUE-1. As MS was located some distance from the dashed line joining OS and S8, the appropriate phase lag was taken into account during fitting. The converging depth contours in CUE-1 introduced a topographic steering effect to the current fluctuations; these topographic phase shifts were assumed to be 37°, 25° and 38°,

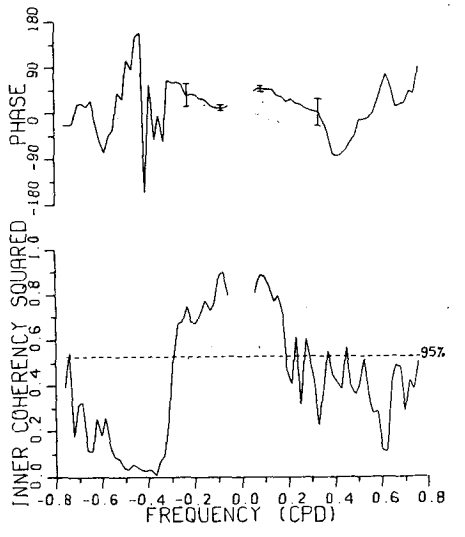

FIG. 8. Cross spectrum between the 60 m current at MS and the 40 m current at NH6.

TABLE 4. Cross-shelf modal fitting on the Washington shelf at selected frequencies, during August–September, 1972.

Frequency (cpd)	Mode	λ (km)	$E_m/\sum E_m$	D
0.16	1	2300	0.88	0.20
	2	750	0.09	
	3	290	0.03	
0.28	1	1300	0.47	0.28
	2	340	0.38	
	3	130	0.14	

clockwise, at the moorings NH10, NH15 and NH20, respectively, and accordingly corrected for in the fitting.

The fits in Tables 4 and 5 were in general not particularly good, the deviation values being quite large. Except for the frequency band at 0.16 cpd in Table 5, the first mode was reasonably prominent in the fits. At 0.16 cpd in Table 5, the deviation value was large (0.40), and the energy was nearly evenly distributed between the first and second modes. Fitting at higher frequencies, 0.45 and 0.67 cpd, was attempted on both shelves, but very poor fits resulted.

4. Discussion

The shelf wave detection techniques developed in H1 have now been applied to several data sets on the Oregon and Washington shelves. The cross-shelf fitting was, in general, most successful on the Oregon shelf data of summer, 1973 (see H1), followed in descending order of success by the 1975 spring and winter data sets, and the 1972 Washington and Oregon shelf data sets. This varying degree of success on the different data sets can probably be explained by the amount of topographic irregularity around the moorings (see Fig. 1). The topographic contours are very regular near the CUE-2 1973 moorings, reasonably regular near the WISP 1975 moorings, quite irregular near the Washington moorings, and very irregular around the CUE-1 1972 moorings. Irregular topography not only makes the computation of theoretical current ellipses uncertain, but more seriously, it introduces wave-scattering. Hence, the cross-shelf fitting technique is only accurate in regions of fairly regular topography. Furthermore, the presence of strong baroclinic fluctuations during winter 1975 (Huyer *et al.*, 1978) decreased the accuracy of the fit (which was based on barotropic theory).

It is generally believed that shelf waves are generated by oscillating wind systems. Theoretical studies were made by Adams and Buchwald (1969) and Gill and Schumann (1974). The Gill and Schumann solution contains shelf waves and a forced wave (which has the same angular frequency ω and wavenumber k as the wind system above). Depending on how the wind-stress forcing is applied, the excited shelf waves may be of the same frequency as the wind but of generally different wavenumbers, or of the same wavenumber as the wind but of different frequencies. The fact that the shelf wave response can be at a frequency different from the forcing frequency allowed Gill and Schumann to explain the observation of Mooers and Smith (1968), where on the Oregon shelf during the summer of 1933, a 0.1 cpd wave moved southward with the atmospheric pressure system, while a 0.35 cpd wave propagated northward like a shelf wave. In fact, this type of propagation pattern seems to occur fairly often on the Oregon shelf. In this study, we have noted that during winter, 1975, and again during early fall, 1972, the propagation at very low frequencies was southward, while at higher frequencies, it was northward, similar to the situation in Mooers and Smith (1968). Chao (1981) has continued the Gill and Schumann study to wind systems of finite extent alongshore.

Recently, Hickey (1981a,b) discarded the traditional shelf-wave explanation for the current fluctuations observed on the Washington and Oregon shelves. The depth-averaged v-momentum equation was taken in her studies to be

$$\frac{\partial v}{\partial t} + \lambda v = \tau/H,$$

where λvH represents linear bottom friction, and τ, the alongshore wind stress. With the Coriolis and horizontal pressure gradient terms discarded, only forced waves are allowed. It is doubtful that the complicated dynamics on the continental shelf could be described properly without the Coriolis force and horizontal pressure gradient terms, which are known to be of substantial magnitudes from the momentum balance studies of Allen and Smith (1981).

It is perhaps unwise to make too sharp a distinction between forced waves and shelf waves, taking them to be unmixable entities. Both arose naturally in the Gill and Schumann solution. There, the forced wave, while copying the (k, ω) values of the wind, depends also on the topography in its cross-shelf structure. On the other hand, the shelf-wave response is determined by the character of the wind. Thus both the

TABLE 5. Cross-shelf modal fitting on the Oregon shelf during July–August, 1972.

Frequency (cpd)	Mode	λ (km)	$E_m/\sum E_m$	D
0.16	1	2600	0.45	0.40
	2	760	0.52	
	3	380	0.02	
0.28	1	1500	0.84	0.25
	2	400	0.16	
	3	200	0.0	

forced wave and the excited shelf waves depend on wind and topography. The cross-shelf structure of the forced wave can actually be expanded as a sum of the free shelf-wave eigenmodes. Hence, the cross-shelf fitting of free wave eigenfunctions indicates how the total kinetic energy—from both the forced wave and the shelf waves—is distributed among the eigenmodes.

As noted in Section 6 of H1, problems are encountered when applying the Gill and Schumann solution to explain the observations on the Oregon shelf. In their linear nondispersive theory, resonance between wind and current is possible only when the wind system is propagating with an alongside phase velocity close to that of a particular shelf-wave mode. During summer 1973, Wang and Mooers (1977, Fig. 6b) found a northward phase speed of 820 km day^{-1} for the atmospheric pressure system on the Oregon shelf, much higher than the phase speeds for the first- and second-mode long shelf waves, (around 350 and 120 km day^{-1}, respectively). Under these circumstances, the Gill and Schumann solution predicts no resonance, but a mixed response consisting of a forced wave and various shelf waves (of decreasing amplitudes with increasing mode number). Examining the distribution of the total kinetic energy (of the forced wave and the shelf waves) by the cross-shelf fitting of free wave eigenfunctions, one would expect to find the energy broadly distributed among the modes, decreasing with increasing mode number. Instead, H1 found that the energy was sharply concentrated in the second eigenmode, in contradiction to the theory. Similarly, the sudden emergence of the third mode in spring 1975 is puzzling. These sudden concentrations of energy into one particular mode certainly suggest some resonant mechanism at work.

In the *linear* theory of Gill and Schumann, resonance between current and wind can occur only when there is a match between the alongshore phase velocity of the wind system and that of a shelf-wave mode. However, the wind systems are often propagating opposite to the direction of shelf waves or at phase speeds that are too high, rendering a linear resonance impossible. Under these circumstances, *nonlinear* resonance between wind and current should be given some consideration.

For nonlinear resonance, the linear resonance condition $(k_1, \omega_1) = (k_2, \omega_2)$ is extended to the more interesting form

$$(k_1, \omega_1) + (k_2, \omega_2) = (k_3, \omega_3), \tag{2}$$

where positive and negative values are allowed for both the wavenumbers and the angular frequencies in this nonlinear resonance condition. Barton (1977) studied a special case of nonlinear shelf-wave generation by the wind, where he took (k_3, ω_3) to denote the forcing wind system, and (k_1, ω_1) and (k_2, ω_2) to be the same shelf wave. Thus

$$(k_1, \omega_1) \equiv (k_2, \omega_2) = \tfrac{1}{2}(k_3, \omega_3). \tag{3}$$

Here the shelf wave generated has half the frequency and wavenumber as the wind system. However, (3) shows that the alongshore phase velocities of the shelf wave and the wind must still be matched.

This restriction on phase velocities can be eliminated by a generalization of Barton's mechanism. We assume the wind (k_3, ω_3) to be generating two different shelf waves (k_1, ω_1) and (k_2, ω_2) under the resonance condition (2). Then the phase velocities of the two shelf waves can be completely different from that of the wind.

Let us suppose that the wind is travelling alongshore with phase speed c. The two shelf waves have different phase speeds represented by

$$\omega_1/k_1 = ac, \quad \omega_2/k_2 = bc, \quad c = \omega_3/k_3\,. \tag{4}$$

Imposing the resonance condition (2), we obtain the relation between the shelf waves and the wind forcing:

$$\left.\begin{aligned}(k_1, \omega_1) &= \frac{1-b}{a-b}(k_3, a\omega_3)\\ (k_2, \omega_2) &= \frac{1-a}{b-a}(k_3, b\omega_3)\end{aligned}\right\}. \tag{5}$$

As an illustration, we consider the situation where the wind is travelling in the same direction as the shelf wave, but at much higher phase speed. In particular, we take $a = \frac{1}{2}$, $b = \frac{1}{8}$, i.e., the two shelf waves propagate at only $\frac{1}{2}$ and $\frac{1}{8}$ of the wind's phase speed, respectively. Eqs. (5) give $\omega_1 = \frac{7}{6}\omega_3$, $k_1 = \frac{7}{3}k_3$, $\omega_2 = -\frac{1}{6}\omega_3$ and $k_2 = -\frac{4}{3}k_3$. [The negative signs in ω_2 and k_2 can be eliminated if we choose the resonance condition to be $(k_1, \omega_1) - (k_3, \omega_3) = (k_2, \omega_2)$.] Hence, the first shelf wave is generated at a frequency close to that of the wind, and the second wave at a much lower frequency. Due to the closeness of ω_1 to ω_3, and the finite band width in a cross spectrum, the coherence between current and wind should be high near ω_3, despite the current propagating at only half the wind's phase speed.

As a second example, we consider a slow-moving wind system travelling opposite to the direction of the shelf waves, and choose $a = -4$, $b = -1$ (negative values in a and b indicate opposite direction of phase propagation from that of the wind). Eqs. (5) give $\omega_1 = \frac{8}{3}\omega_3$, $k_1 = -\frac{2}{3}k_3$, $\omega_2 = -\frac{5}{3}\omega_3$, $k_2 = \frac{5}{3}k_3$, i.e., both waves are generated at somewhat higher frequencies than that of the wind.

These examples illustrate the versatility of the nonlinear resonance. We can also estimate the time scales and length scales for the nonlinear resonance to develop.

The importance of nonlinearity is often characterized by ϵ, the ratio of the magnitude of the inertial term uv_x to that of the Coriolis term fu in the along-

shore momentum equation. Thus

$$\epsilon = \frac{V}{Lf},$$

where V/L characterizes the velocity gradient. If V is taken to be the magnitude of the alongshore velocity near the coast ($V = 10^{-1}$ m s^{-1}), then for the first mode, L can be taken to be the shelf width ($\sim$100 km). However, for the higher modes, we should let L be the distance from the coast to the first node of the alongshore velocity. From Fig. 4a in H1, L = 33 and 26 km for the second and third modes, respectively. Thus, at mid-latitudes ($f \approx 10^{-4}$ rad s^{-1}), ϵ = 0.010, 0.030 and 0.038 for the first, second and third modes. The time scale for the nonlinear interactions is characterized by $T = (\epsilon f)^{-1}$ (Barton, 1977, Section 6; Hsieh and Mysak, 1980, p. 1739), which comes to 12 days, 3.8 days and 3.0 days for the first, second and third modes.

The alongshore extent of the wind-forcing region required for substantial nonlinear energy transfer is characterized by a length scale Y ($Y = cT$), the distance covered by the waves propagating at phase speed c in time T. With c having the values 350, 120 and 55 km day^{-1} for the first, second and third modes, respectively, Y takes on the corresponding values 4000, 450 and 170 km.

The large time and length scales, T and Y, for the first mode suggest that the nonlinear transfer from wind to the first mode is probably insignificant. On the other hand, the much shorter T and Y scales for the second and third modes imply that the nonlinear excitation of these modes is possible. The nonlinear mechanism actually favors the higher modes to the first mode, i.e., if the wind forms a resonant triad with a first mode and a higher mode, the higher mode will probably emerge much more prominently than the first mode in the current data, as observed frequently.

The sudden emergence of the third mode during spring 1975 may also be related to the change in the shelf water stratification. How changes in the stratification affect the wind excitation of shelf waves has not yet been investigated. The full problem of how atmospheric fluctuations transfer energy, both linearly and nonlinearly, into current fluctuations on the continental shelf, under various stratification conditions, is still far from being solved.

5. Summary and conclusions

The nature of the current fluctuations on the Oregon shelf changed drastically from winter to spring, 1975. At low frequencies the offshore energy decay rate of the current fluctuations was much faster, and the alongside propagation speed much slower, in spring than in winter. These observations were consistent with the excitation of a higher shelf wave mode in spring. Detailed cross-shelf study showed that in a frequency band around 0.16 cpd, the dominance of the first mode shelf wave in winter was terminated by the emergence of the third mode in spring. At very low frequencies ($\leqslant$0.1 cpd), the current fluctuations propagated southward in winter, opposite to the direction of shelf waves.

On the Oregon and Washington shelves during summer (and early fall) 1972, the location of moorings in regions of very irregular topography rendered the task of data interpretation much more difficult. Nevertheless, the rapid northward propagation, the slow offshore energy decay, and the cross-shelf fitting generally agreed with the presence of the first shelf-wave mode. The observed phase speed, being somewhat larger than that of the first mode shelf wave, could be caused by either the presence of a forced wave or phase distortion by irregular topography. By early fall, 1972, a southward propagation developed at very low frequencies. In contrast, the current fluctuations on the Oregon shelf during the following summer (1973) were found to display clearly the characteristics of the second mode shelf wave.

It has been known from past observations on the Oregon and Washington shelves that the properties of the current fluctuations—the offshore energy decay rate, the current ellipse patterns and the alongshore propagation speed—all vary dramatically with time. This paper and its predecessor H1 have demonstrated that these properties are by no means mutually unrelated, but are closely connected as manifestations of propagating shelf waves. For instance, a substantial decrease in the alongshore propagation speed occurred simultaneously with a more rapid offshore energy decay during the emergence of the third mode in spring, 1975. Furthermore, the dramatic changes in the nature of the current fluctuations can be interpreted as merely a reflection of different shelf-wave modes being excited at different times. Thus shelf waves provide a unifying and fruitful approach to current fluctuation phenomena on the continental shelf.

The emergence of relatively high modes (modes 2 and 3) is surprising. That this can happen quickly, with the current energy sharply concentrated into one particular mode, is even more remarkable, and strongly hints at a resonance mechanism at work. Unfortunately, it is not clear how these higher mode waves are generated. The present shelf-wave generation theories require, for resonance response, a matching of the alongshore phase velocity of the wind system and that of a shelf wave—a condition that is often difficult to satisfy, at least on the Oregon and Washington shelves. Nonlinear resonance between wind and current does not impose this constraint, and in addition, actually favors the higher modes to the first mode, thereby providing a promising mechanism for the generation of these higher mode shelf waves.

Acknowledgments. I sincerely thank Dr. A. Huyer of the Oregon State University at Corvallis for providing the Oregon shelf data, and Dr. B. M. Hickey of the University of Washington for the Washington shelf data. I am also indebted to Professor L. A. Mysak, who supervised my doctoral dissertation. This work was supported by the Natural Sciences and Engineering Research Council of Canada, and was typed in the Department of Applied Mathematics and Theoretical Physics at the University of Cambridge.

REFERENCES

Adams, J. K., and V. T. Buchwald, 1969: The generation of continental shelf waves. *J. Fluid Mech.*, **35,** 815–826.

Allen, J. S., and R. L. Smith, 1981: On the dynamics of wind-driven shelf currents. *Phil. Trans. Roy. Soc. London*, **A302,** 617–634.

Barton, N. G., 1977: Resonant interactions of shelf waves with wind-generated effects. *Geophys. Astrophys. Fluid Dyn.*, **9,** 101–114.

Chao, S.-Y., 1981: Forced shelf circulation by an alongshore wind band. *J. Phys. Oceanogr.*, **11,** 1325–1333.

Gill, A. E., and E. H. Schumann, 1974: The generation of long shelf waves by the wind. *J. Phys. Oceanogr.*, **4,** 83–90.

Hickey, B. M., 1981a: Alongshore coherence on the Pacific Northwest continental shelf (January–April 1975). *J. Phys. Oceanogr.*, **11,** 822–835.

——, 1981b: Temporal and spatial variability of the California undercurrent off Washington during summer 1972. Submitted to *J. Mar. Res.*

Hsieh, W. W., 1982: On the detection of continental shelf waves. *J. Phys. Oceanogr.*, **12,** 414–427.

——, and L. A. Mysak, 1980: Resonant interactions between shelf waves, with applications to the Oregon shelf. *J. Phys. Oceanogr.*, **10,** 1729–1741.

Huyer, A., B. M. Hickey, J. D. Smith and R. D. Pillsbury, 1975: Alongshore coherence at low frequency in currents observed over the continental shelf off Oregon and Washington. *J. Geophys. Res.*, **80,** 3495–3505.

——, R. L. Smith and E. J. C. Sobey, 1978: Seasonal differences in low-frequency current fluctuations over the Oregon continental shelf. *J. Geophys. Res.*, **83,** 5077–5089.

Jenkins, G. M., and D. G. Watts, 1968: *Spectral Analysis and Its Applications.* Holden-Day, 525 pp.

Kundu, P. K., and J. S. Allen, 1976: Some three-dimensional characteristics of low-frequency current fluctuations near the Oregon coast. *J. Phys. Oceanogr.*, **6,** 181–199.

——, —— and R. L. Smith, 1975: Modal decomposition of the velocity field near the Oregon coast. *J. Phys. Oceanogr.*, **5,** 683–703.

Mooers, C. N. K., and R. L. Smith, 1968: Continental shelf waves off Oregon. *J. Geophys. Res.*, **73,** 549–557.

Wang, D.-P., 1980: Diffraction of continental shelf waves by irregular alongshore geometry. *J. Phys. Oceanogr.*, **10,** 1187–1199.

——, and C. N. K. Mooers, 1977: Long coastal-trapped waves off the west coast of the United States, summer 1973. *J. Phys. Oceanogr.*, **7,** 856–864.